Cell Reports Medicine, Volume *4*

Supplemental information

Conserved angio-immune subtypes of the tumor microenvironment predict response to immune checkpoint blockade therapy

Madhav Subramanian, Ashraf Ul Kabir, Derek Barisas, Karen Krchma, and Kyunghee Choi

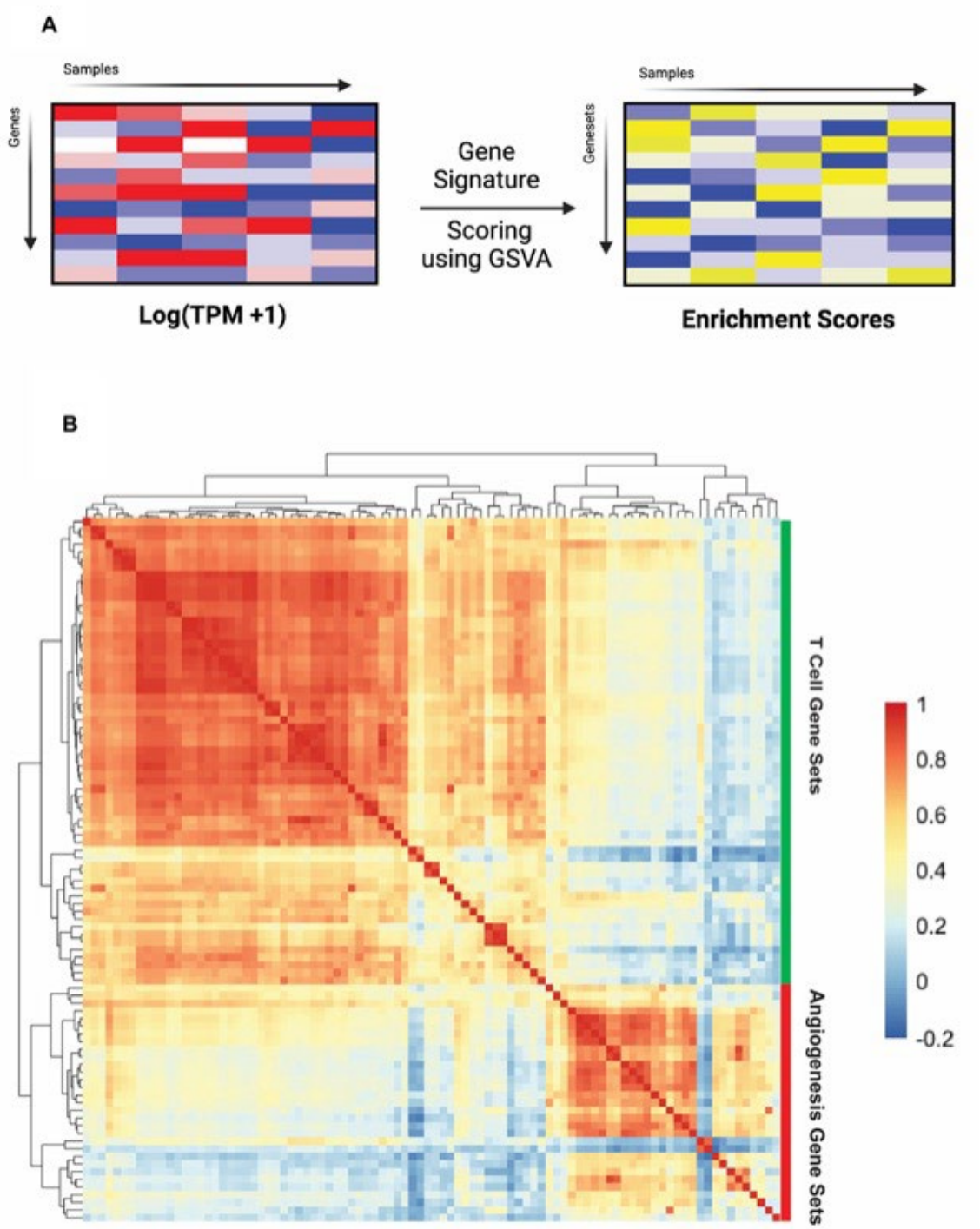

Figure S1. Three pan cancer angio-immune subtype identification (Supplemental Information for Figure 1).

A) Schematic depicting generation of enrichment matrices used for angio-immune subtype identification. RNA-sequencing data was used to score the enrichment of 91 gene signatures using GSVA. Results of GSVA are used to identify angio-immune subtypes.

B) Heatmap depicting Pearson correlation of gene sets across 11,069 TCGA tumor samples. Gene sets are bound by positive correlation and separated by negative correlation.

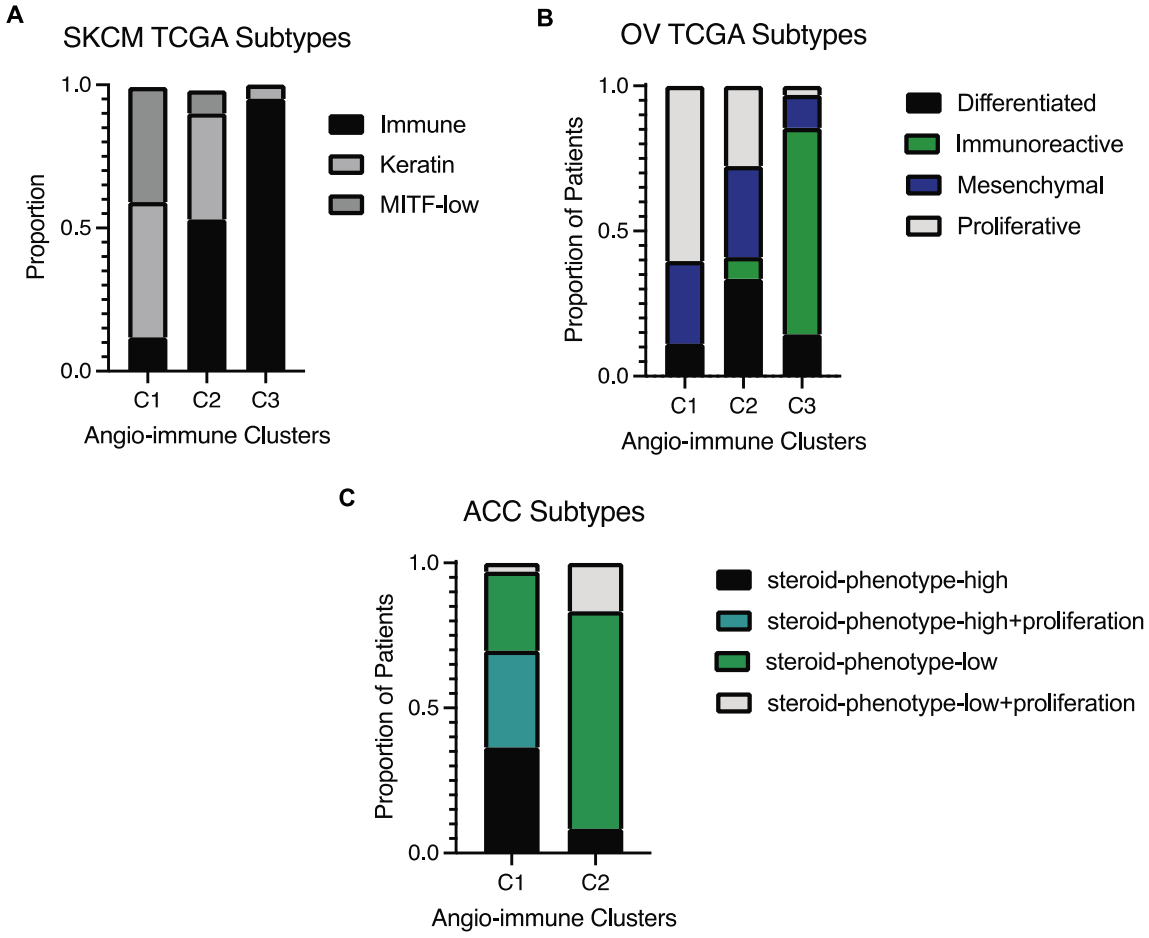

Figure S2. Pan-cancer clustering is fair to individual tumor types (Supplemental Information for Figure 1).

A) Comparison of membership to previously established molecular subtypes and angio-immune clusters in skin cutaneous melanoma (SKCM).

B) Comparison of membership to previously established molecular subtypes and angio-immune clusters in ovarian carcinoma (OV).

C) Comparison of membership to previously established molecular subtypes and angio-immune clusters in adrenocortical carcinoma (ACC).

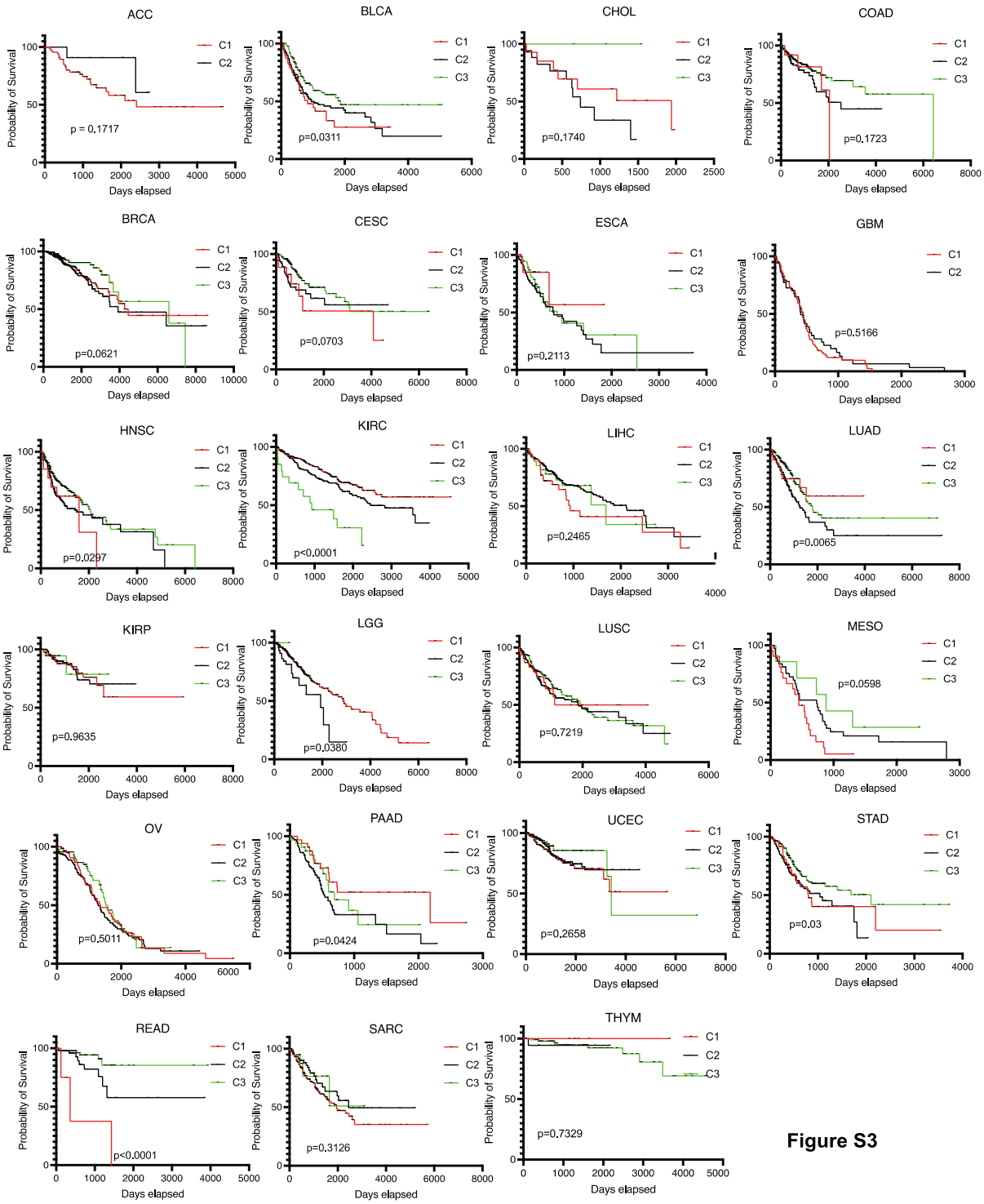

Figure S3

Figure S3. Overall survival of TCGA tumors (Supplemental Information for Figure 1). Overall survival for tumor types among patients belonging to the three angio-immune clusters. Survival differences observed in bladder adenocarcinoma (BLCA), lung adenocarcinoma (LUAD), head and neck squamous cell carcinoma (HNSC), clear cell renal carcinoma (KIRC), low grade glioma (LGG), pancreatic adenocarcinoma (PAAD), stomach adenocarcinoma (STAD), and renal adenocarcinoma (READ).

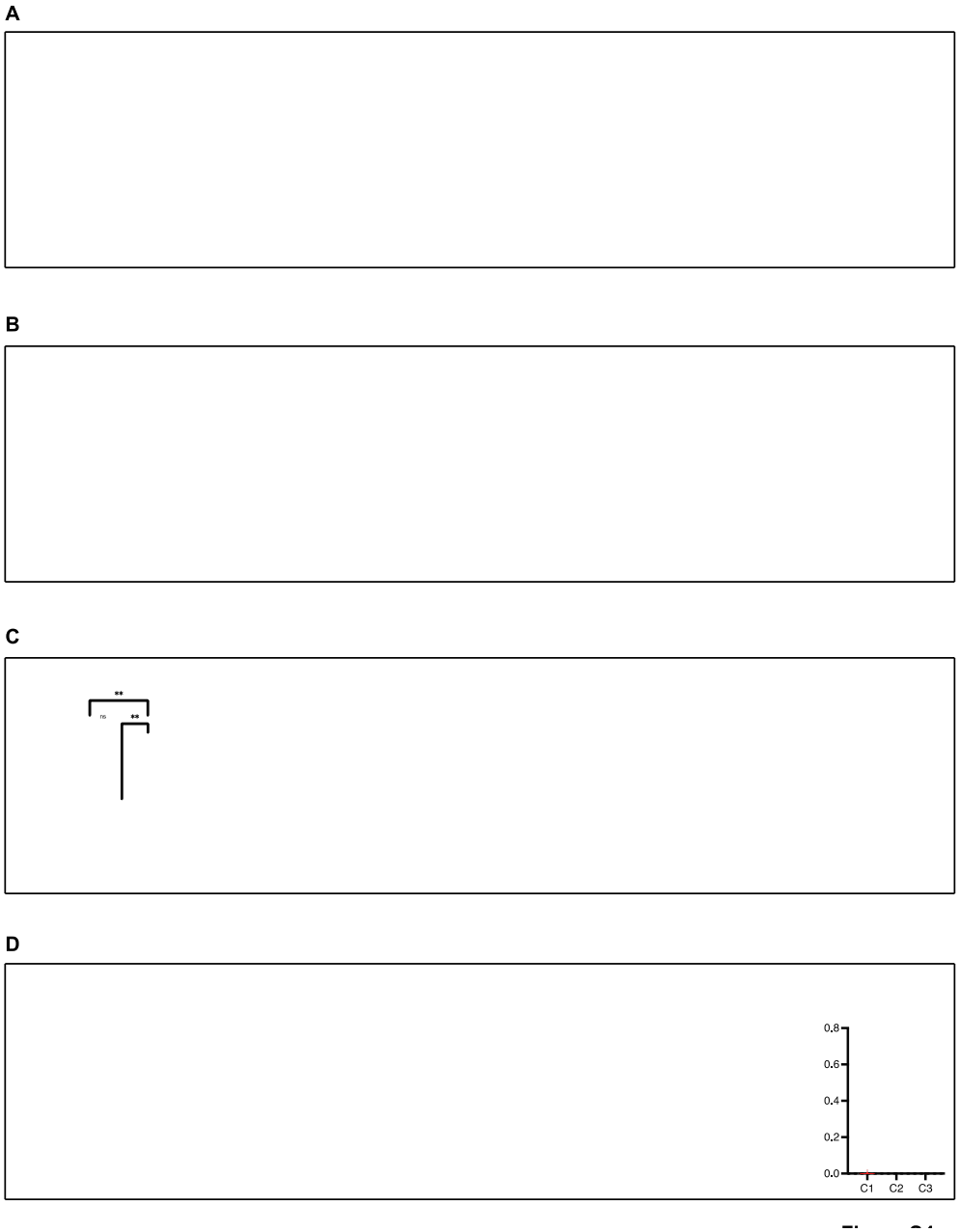

Figure S4. Distinct mutations characterize angio-immune clusters in specific tumor types (Supplemental information for Figure 2).

A) Oncoplot depicting mutation frequency across angio-immune clusters in skin cutaneous melanoma. Plots were generated using the maftools package. Publicly available mutation annotation files from the GDC pancancer atlas was used to derive the data.

B) Oncoplot depicting mutation frequency across angio-immune clusters in bladder adenocarcinoma. Plots were generated using the maftools package. Publicly available mutation annotation files from the GDC pancancer atlas was used to derive the data.

C) Oncoplot depicting mutation frequency across angio-immune clusters in stomach adenocarcinoma. Plots were generated using the maftools package. Publicly available mutation annotation files from the GDC pancancer atlas was used to derive the data.

D) Oncoplot depicting mutation frequency across angio-immune clusters in renal cell carcinoma. Plots were generated using the maftools package. Publicly available mutation annotation files from the GDC pancancer atlas was used to derive the data.

*=p<0.05, **=p<0.01, ***=p<0.001, ****=p<0.0001

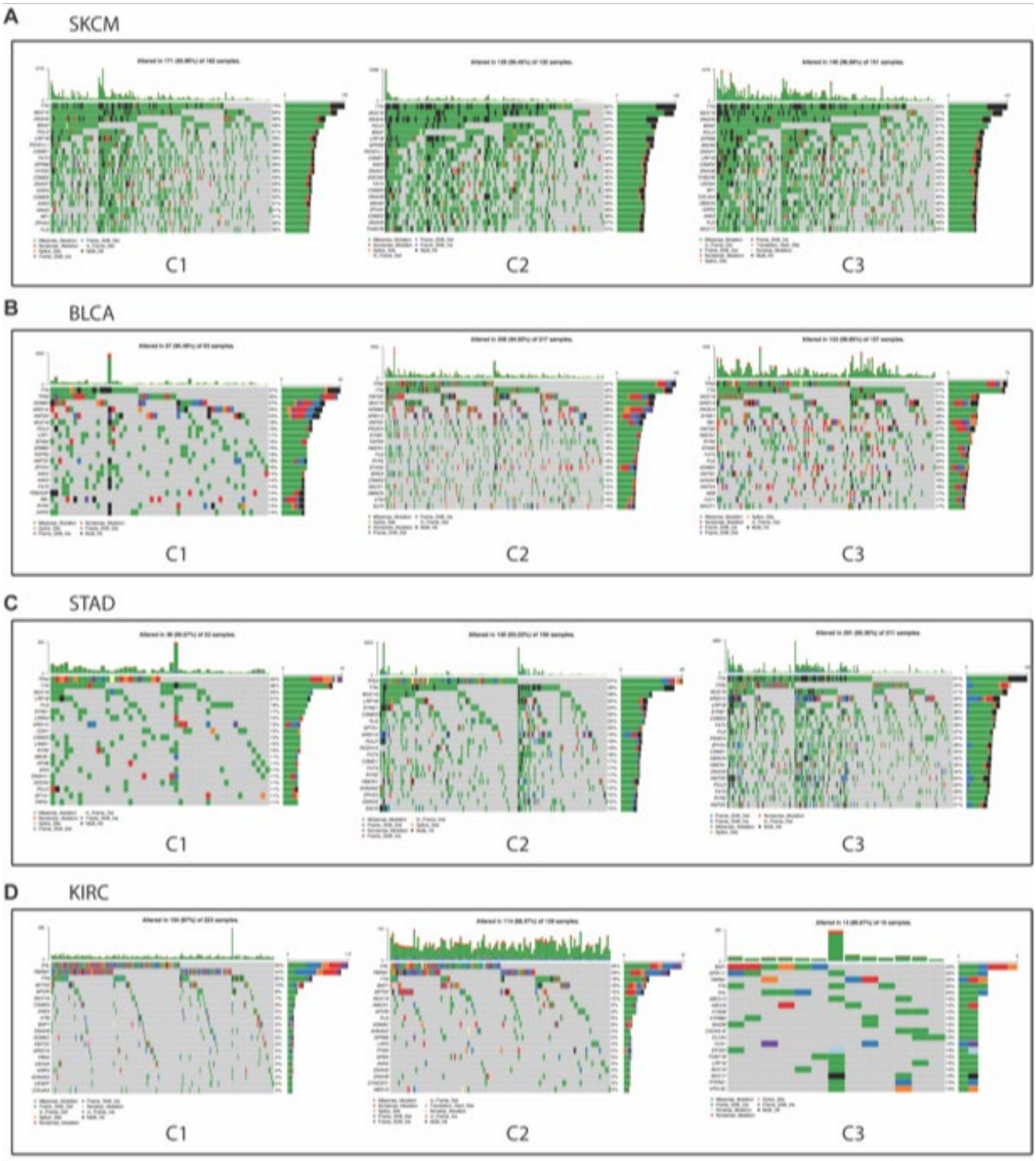

Figure S5. Immune cell infiltration analysis for individual tumor types are consistent with reported pan-cancer phenotypes (Supplemental information for Figure 2).

A) Violin plots showing xCell enrichment results of CD8 T cell, M1 macrophage, classical dendritic cell (cDC), B cells, Th1 cells, and Th2 cells across angio-immune subtypes among skin cutaneous melanoma patients from the TCGA. One way ANOVA was used to determine statistical significance.

B) Violin plots showing xCell enrichment results of CD8 T cell, M1 macrophage, classical dendritic cell (cDC), B cells, Th1 cells, and Th2 cells across angio-immune subtypes among bladder cancer patients from the TCGA. One way ANOVA was used to determine statistical significance.

C) Violin plots showing xCell enrichment results of CD8 T cell, M1 macrophage, classical dendritic cell (cDC), B cells, Th1 cells, and Th2 cells across angio-immune subtypes among stomach adenocarcinoma patients from the TCGA. One way ANOVA was used to determine statistical significance.
D) Violin plots showing xCell enrichment results of CD8 T cell, M1 macrophage, classical dendritic cell (cDC), B cells, Th1 cells, and Th2 cells across angio-immune subtypes among clear cell renal carcinoma patients from the TCGA. One way ANOVA was used to determine statistical significance.

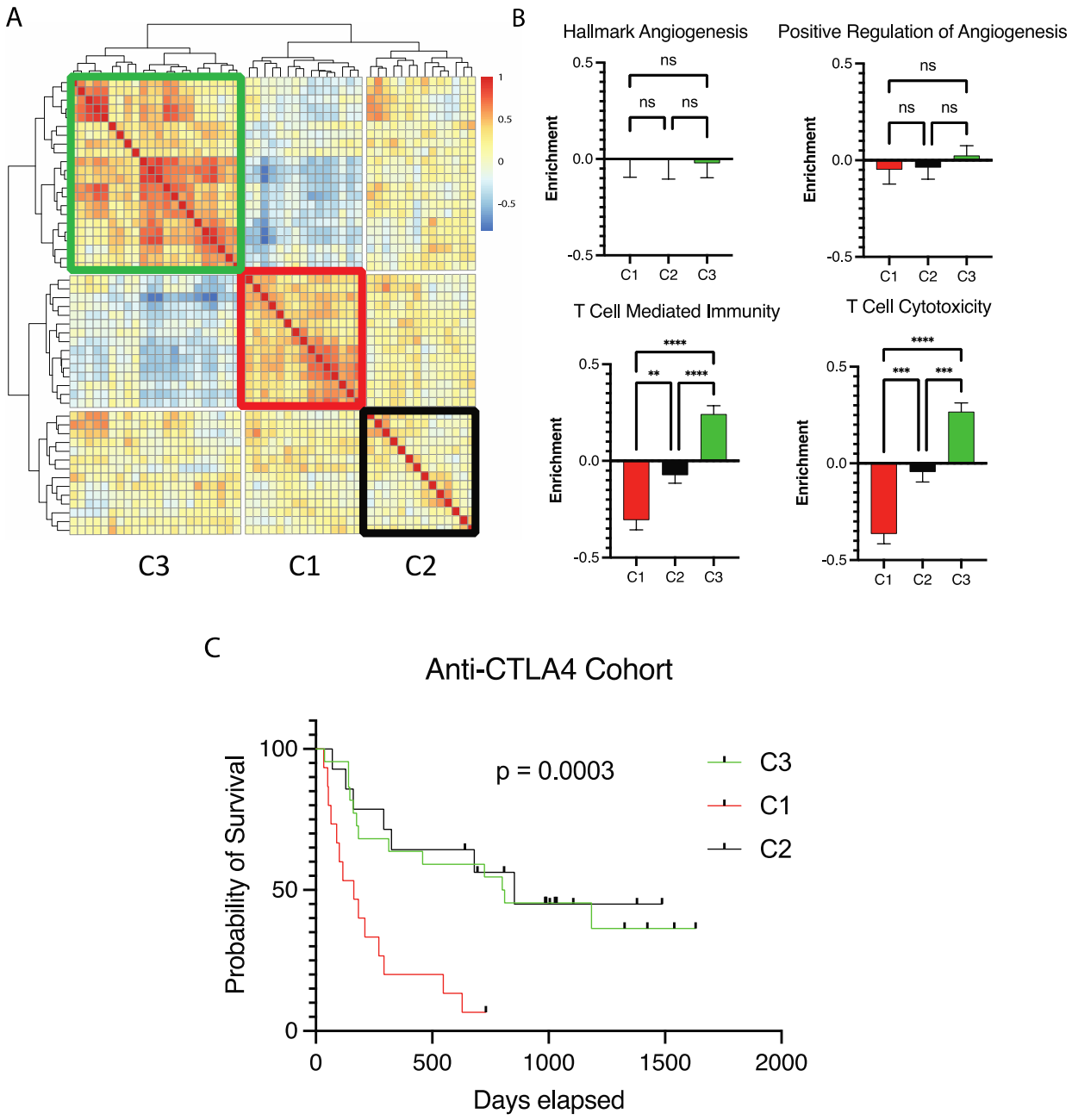

Figure S6. Analysis of anti-CTLA4 treated melanoma (Supplemental information for Figure 3).

A) Heatmap of Pearson Correlation of 51 patients with Melanoma treated with anti-CTLA4 across 91 gene sets corresponding T-cell and angiogenesis activity. Angio-immune subtypes were conserved in this melanoma cohort.

B) Bar graphs depicting the average enrichment of angiogenesis signature and T-cell signature in the three angio-immune subtypes in the anti-CTLA4 treated Melanoma cohort. One way ANOVA was used to determine statistical significance.

C) Overall survival for patients in different angio-immune clusters upon treatment with anti- CTLA4 in melanoma patients.

*=p<0.05, **=p<0.01, ***=p<0.001, ****=p<0.0001

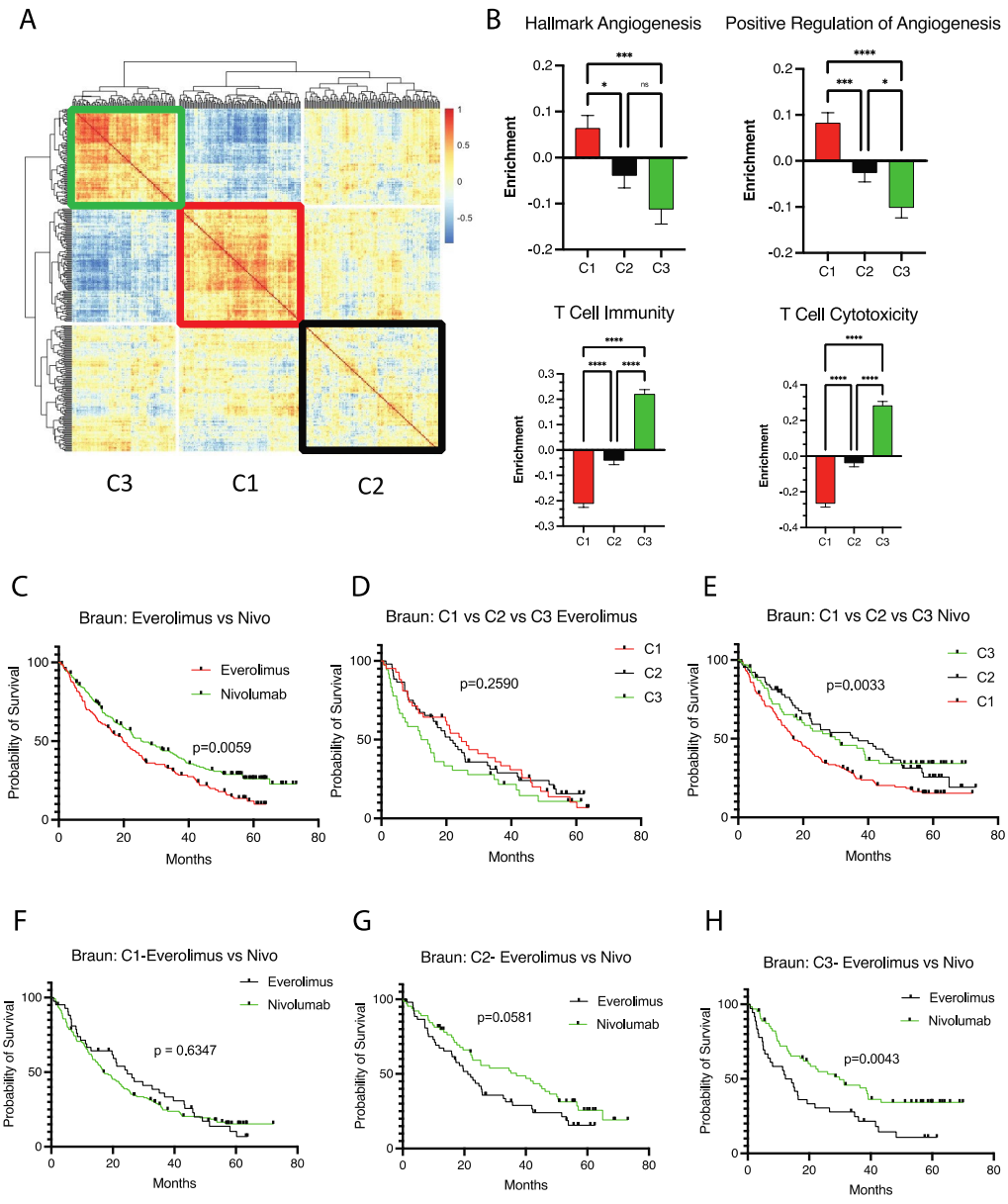

Figure S7. Re-evaluation of Checkmate010 and Checkmate025 (Braun) reveals differing propensity for response by angio-immune subtypes (Supplemental information for Figure 4).

A) Heatmap of Pearson Correlation of 311 patients with Renal Cell Carcinoma across 91 gene sets corresponding T-cell and angiogenesis activity. Angio-immune subtypes were conserved in this renal cancer cohort.

B) Bar graphs depicting the average enrichment of angiogenesis signatures and T-cell signatures in the three angio-immune subtypes in the Braun Renal Cell Carcinoma cohort. One way ANOVA was used to determine statistical significance.

C) Overall survival of patients treated with everolimus vs nivolumab

D) Overall survival of patients treated with everolimus belonging to different angio-immune clusters

E) Overall survival of patients treated with nivolumab belonging to different angio-immune clusters

F) Overall survival of patients belonging in C1 treated with everolimus vs nivolumab

G) Overall survival of patients belonging in C2 treated with everolimus vs nivolumab

H) Overall survival of patients belonging in C3 treated with everolimus vs nivolumab

*=p<0.05, **=p<0.01, ***=p<0.001, ****=p<0.0001

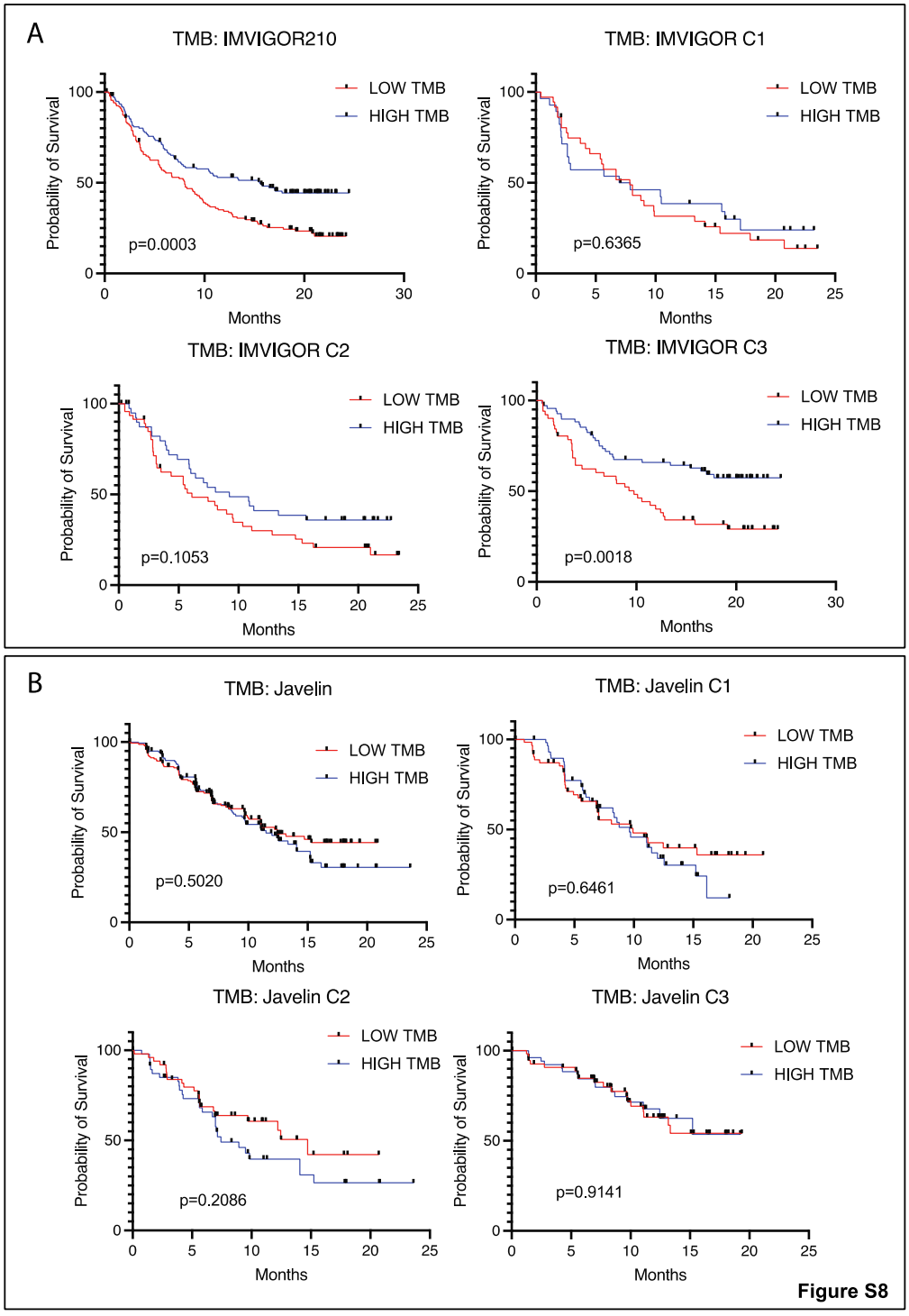

Figure S8. Re-evaluating tumor mutational burden as a predictor of response (Supplemental information for Figure 5).

A) Overall survival of anti-PDL1 treated bladder cancer patients separated by tumor mutational burden status. Survival was plotted for patients across the cohort and belonging to the three angio-immune clusters separated by high (>50th percentile) and low (<50th percentile) tumor mutational burden.

B) Progression-free survival of anti-PDL1 treated renal cancer patients separated by tumor mutational burden status. Survival was plotted for patients across the cohort and patients belonging to the three angio-immune clusters separated by high (>50th percentile) and low (<50th percentile) tumor mutational burden